

Change of Chemical Species with Progress of Crevice Corrosion

Lizhu Tong^{1*} and Masahiro Yamamoto²

¹ Keisoku Engineering System Co., Ltd., 1-9-5 Uchikanda, Chiyoda-ku, Tokyo 101-0047, Japan

² Japan Atomic Energy Agency, 2-2-2 Uchisaiwaicho, Chiyoda-ku, Tokyo 100-8577, Japan

*Corresponding author: tong@kesco.co.jp

Abstract: This paper presents a model research on change of chemical species with progress of crevice corrosion of stainless steel SUS304 in NaCl solution. The reversible reactions specifying equilibrium constants in the Chemistry interface of COMSOL Multiphysics® are used to solve the equilibrium reactions occurred in the solution, which are coupled with the Tertiary Current Distribution, Nernst-Planck interface. The approach is verified to be efficient in calculating the transport of various chemical species and the chemical reactions occurred in the crevice. The solution properties with the progress of crevice corrosion are examined.

Keywords: Crevice corrosion, Equilibrium reactions in solution, pH value, O₂ concentration, Numerical analysis

Introduction

One of the most destructive modes for corrosion of metals is localized corrosion. This can take many forms depending on the chemical and electrochemical environment of the metal. One important form is crevice corrosion [1,2], which occurs where two or more surfaces in close proximity lead to the creation of a locally occluded region. The narrow region makes exchange of solution between the interior and the bulk difficult. It is known that during crevice corrosion, metal dissolves at a large current density associated with the electrochemical reaction, which causes the solution composition, pH, and dissolved oxygen concentration to exceedingly vary [3,4]. Typically, the width of crevice is several tens of μm or less, which is so narrow that it is difficult to make an experimental measurement of the environmental factors. Therefore, the numerical analysis technique is highly efficient [5,6].

In this work, we present a simulation research based on a two-dimensional model of crevice corrosion of stainless steel SUS304 in NaCl solution. The equilibrium reactions occurred in the solution are combined with the electrochemical reactions on the surface of SUS304. The concentration distributions of various ions, oxygen, and hydrogen in the crevice are obtained and the pH value in the crevice is presented and evaluated.

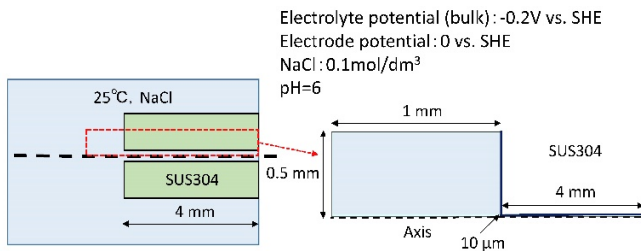


Figure 1. Specimen configuration of crevice corrosion and computational model.

Numerical Model

The layout of 2D configuration of a crevice used in this work is shown in Fig. 1. Since the width of crevice, distance between two SUS304 sheets, is several tens of μm or less and the depth of crevice is more than 10 mm, it is appropriate to consider the present research in a 2D model. In this work, the central axis of the crevice is considered as the symmetry axis of a 2D axis-symmetrical model, in which the half width of crevice is 10 μm. A solution layer with thickness of 0.5 mm is taken into account, which is consistent with that of diffusion layer at room temperature. 0.1 M Sodium Chloride Solution (NaCl) is considered. The chemical species taken into account in the solution are Fe²⁺, Ni²⁺, Cr³⁺, H⁺, OH⁻, FeOH⁺, CrOH²⁺, FeCl⁺, CrCl²⁺, CrClOH⁺, Na⁺, Cl⁻, O₂, H₂, H₂O. The initial pH is 6. The equation for transport of chemical species in the solution, subject to diffusion and electromigration is [7,8]

$$\frac{\partial c_i}{\partial t} + \nabla \cdot (-D_i \nabla c_i - z_i u_{m,i} F c_i \nabla \phi_l + c_i \mathbf{u}) = R_i, \quad (1)$$

where c_i is the concentration of species i , D_i is the diffusion coefficient of species i , z_i is the charge number of species i , $u_{m,i}$ is the mobility of species i , F is the Faraday's constant, ϕ_l is the potential, \mathbf{u} is the fluid velocity, and R_i is the reaction rate. Since fluid flow is not calculated in this work, $\mathbf{u} = 0$.

The current density \mathbf{i} in the solution is

$$\mathbf{i}_l = F \sum_i z_i (-D_i \nabla c_i - z_i u_{m,i} F c_i \nabla \phi_l), \quad (2)$$

$$\nabla \cdot \mathbf{i}_l = 0. \quad (3)$$

Also, an electroneutrality condition is considered by

$$\sum_i z_i c_i = 0. \quad (4)$$

It is known that in general, the chemical reactions in the solution can be calculated by the equilibrium constants, but during the corrosion in a crevice, various metal ions are dissolved and local concentration in the crevice changes rapidly. When the width of crevice is quite narrow, e.g., 20 μm, it will be difficult to reach an equilibrium state in the initial stage of crevice corrosion, which causes a serious convergence issue. Therefore, in this work the reversible reactions specifying equilibrium constants are taken into account [6]

$$r_j = k_j^f \prod_{i \in \text{react}} c_i^{-v_{i,j}} - k_j^r \prod_{i \in \text{prod}} c_i^{v_{i,j}}, \quad (5)$$

where r_j is the reaction rate of reaction j , k_j^f and k_j^r are the forward and reverse rate constants, respectively, $v_{i,j}$ is the stoichiometric coefficient, which is defined as being negative for reactants (*react*) and positive for products (*prod*). The equilibrium reactions and reaction constants taken into account in this work are shown in Table 1. The equilibrium constants K_{eq} are obtained by converting the equilibrium constants for the conventional 1 L (1 M = 1 mol/dm³) to 1 m³ [4,6]. K^f is the

Table 1: Equilibrium reactions and reaction constants

No.	Reaction	K_{eq}	K^r
r1	$H_2O \leftrightarrow OH^- + H^+$	1.8×10^{-13}	1×10^{-12}
r2	$Cr^{3+} + H_2O \leftrightarrow CrOH^{2+} + H^+$	2.27×10^{-6}	1×10^{-5}
r3	$Cr^{3+} + Cl^- \leftrightarrow CrCl^{2+}$	1.91×10^{-3}	1×10^{-4}
r4	$CrCl^{2+} + H_2O \leftrightarrow CrClOH^+ + H^+$	1.0×10^{-5}	1×10^{-7}
r5	$Fe^{2+} + H_2O \leftrightarrow FeOH^+ + H^+$	1.81×10^{-12}	1×10^{-14}
r6	$Fe^{2+} + Cl^- \leftrightarrow FeCl^+$	4.29×10^{-3}	1×10^{-6}

forward rate constant, and the reverse rate constant K^r is equal to K^f/K_{eq} .

Electrochemical kinetics at the electrode can be described by polarization data, which represent a relationship between the local current density and the local overcharge at the electrode. Dissolution of SUS304 occurs in a crevice according to

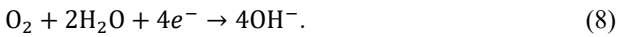


In calculation, the three reactions are replaced by the dissolution of single metal atom M [6]

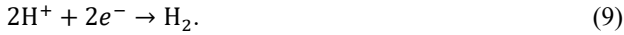


where n is the number of participating electrons. The contents of elements in SUS304 are 0.716, 0.197 and 0.087 for Fe, Cr, and Ni, respectively. Thus, $n = 2 \times 0.716 + 3 \times 0.197 + 2 \times 0.087 = 2.2$. In this work, three kinds of polarization curves for dissolution of SUS304, passive, active 1 and active 2, are used as shown in Fig. 2. The passive curve is the measured value on the passive film of SUS304. It is assumed that the active state occurs inside the crevice with a high current density in the entrance and a low current density in the interior of crevice, which correspond to polarization curves, active 1 and active 2. For the active 2, the current density of polarization curve is considered as 1000 times of that of the passive curve and the current density of active 1 is 5 times of that of the active 2.

The reduction reaction of dissolved oxygen is described by [6]



Recently, the effect of evolution of hydrogen on crevice corrosion has been reported [9]. In this work, the evolution of hydrogen is also included [10]

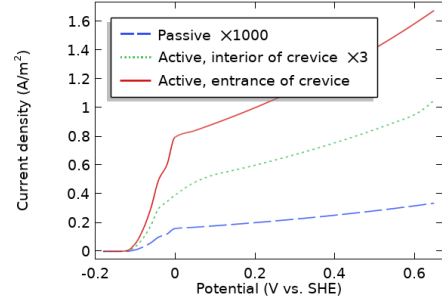


The reduction reactions shown in eqs. (8) and (9) are solved by the Tafel approximation [11]

$$i_{loc} = -i_0 \times 10^{\eta/A_c}, \quad (10)$$

where i_{loc} is the local current density at SUS304, i_0 is the exchange current density, A_c is the Tafel slope, η is the overvoltage, which is the potential difference between the electrode potential, V , the solution potential adjacent to the electrode, ϕ_0 , and equilibrium potential, $E_{eq,S}$, i.e., $\eta = V - \phi_0 - E_{eq,S}$. The subscript S denotes O_2 or H_2 . In this work, $i_0 = i_{0,S} \times (c_S/c_{S,bulk})^\gamma$ [12], in which $i_{0,S}$ is the exchange current density without the effect of species concentration, c_S is the surface concentration of electrode, $c_{S,bulk}$ is the bulk concentration in solution. γ is the factor representing the effect

of concentration on current density, which is taken 1 and 2 for the reduction reactions shown in eqs. (8) and (9), respectively.

**Figure 2.** Polarization curves for SUS304 in NaCl solution.

Simulation Results

1) Benchmark study of equilibrium reactions occurred in the solution of crevice corrosion

In order to evaluate the solution properties of corrosion in a crevice, it is necessary to embed the main chemical equilibrium reactions occurred in solution in the simulation of crevice corrosion. In this work, these equilibrium reactions are confirmed by a benchmark simulation in comparison of the simulation results with the experimental data [4]. The calculation is performed for a solution involving $FeCl_2 \cdot 4H_2O$, $CrCl_3 \cdot 6H_2O$ and $NiCl_2 \cdot 6H_2O$ in a 2D area of $2\text{ cm} \times 2\text{ cm}$, which is consistent with the experimental set-up. The equilibrium reactions and reaction constants shown in Table 1 are used. The simulation time considered in this work is set to 10 hours so that a complete equilibrium state is considered to be achieved.

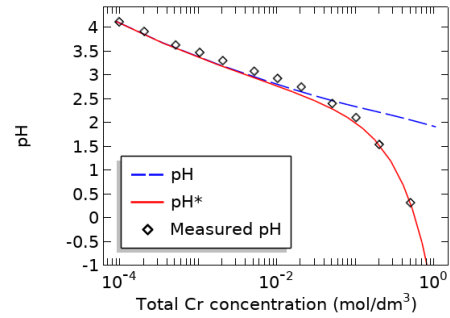
**Figure 3.** pH and its modified value pH* by activity coefficient in comparison with the experiment data.

Figure 3 shows the simulated pH in comparison with the experiment values. It is noted that the simulated pH is higher than the experimental values at $pH < 2.5$, which has been deduced to a fact that the effect of activity coefficient becomes important at $pH < 2.5$ [4,13].

$$\log Y_{all} = \log Y_{FeCl_2} + \log Y_{CrCl_3} + \log Y_{NiCl_2},$$

$$pH^* = -\log (c_{H^+} Y_{all}),$$

where Y_{FeCl_2} , Y_{CrCl_3} , and Y_{NiCl_2} denote the increasing ratios of activity coefficient of H^+ with $FeCl_2$, $CrCl_3$, $NiCl_2$ species, respectively, and Y_{all} is the sum of the increasing ratios of activity coefficient of H^+ for each chemical species. c_{H^+} is the

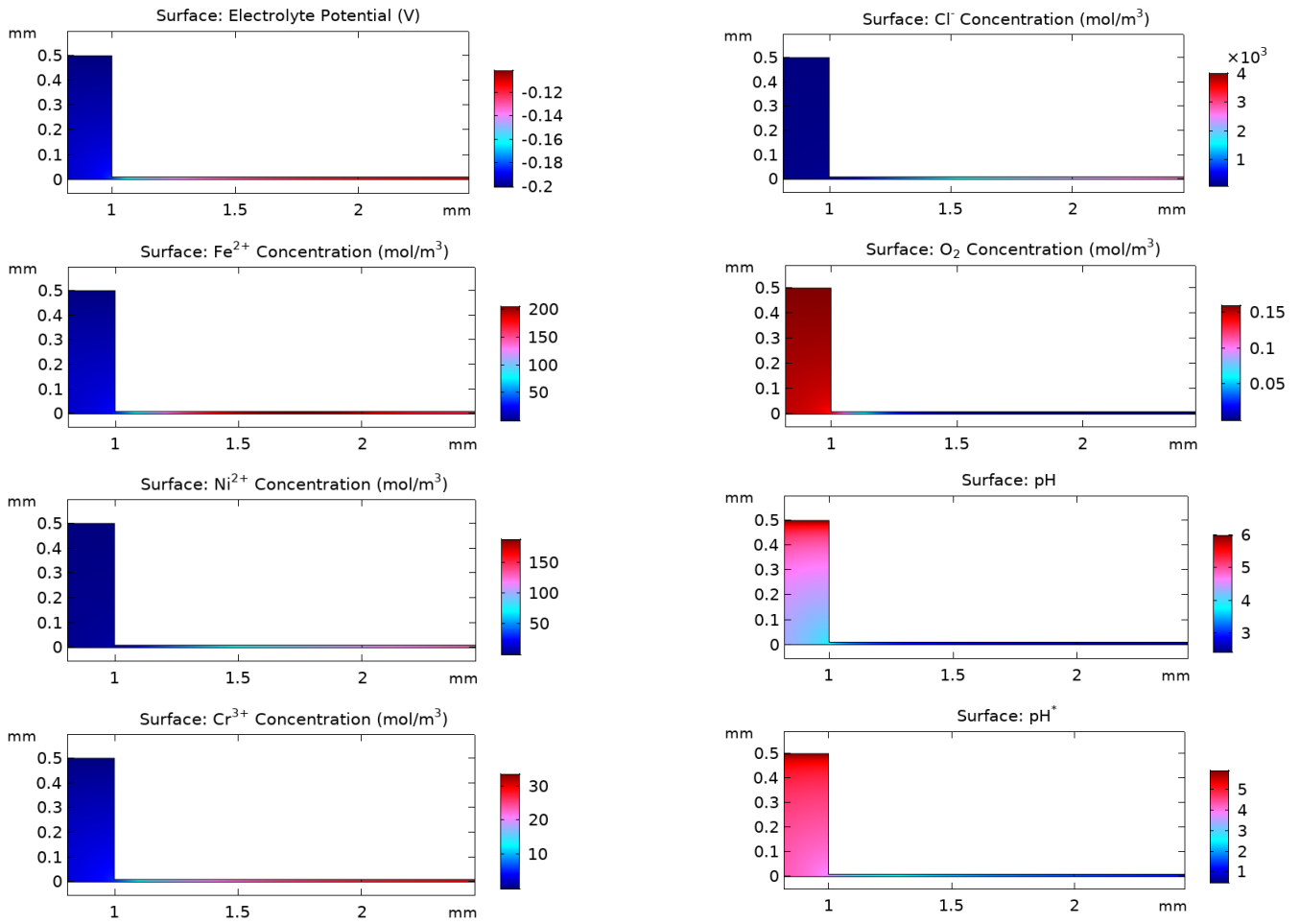


Figure 4. Distributions of potential, concentrations of Fe²⁺, Ni²⁺, Cr³⁺, Cl⁻ ions and O₂, pH and pH* in a crevice.

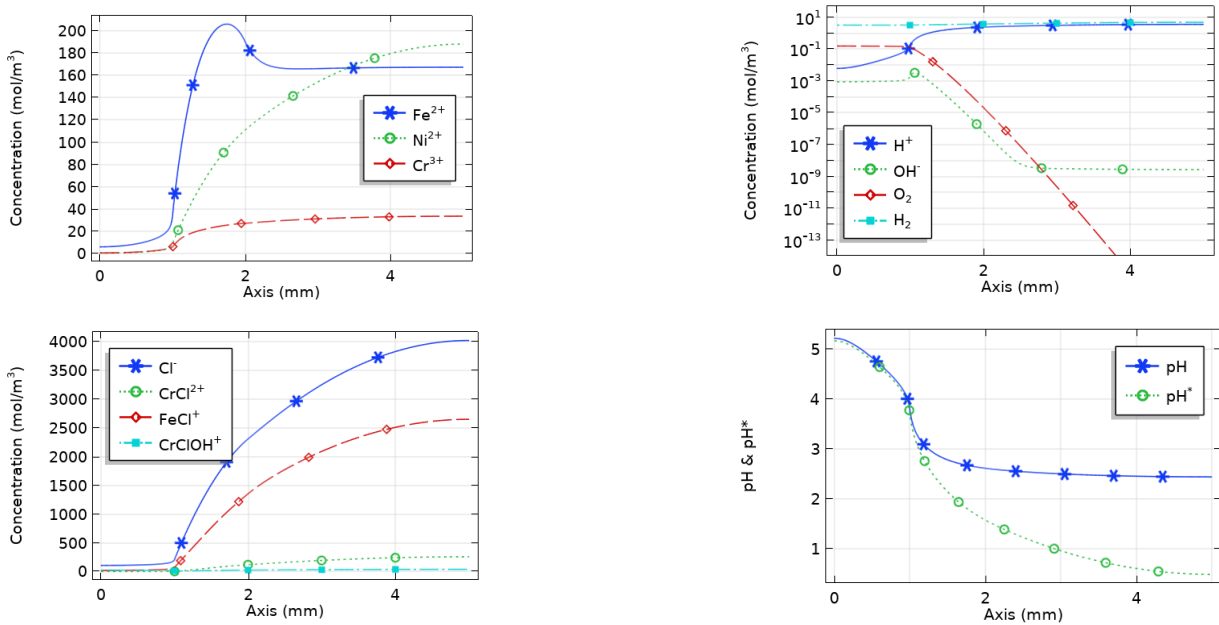


Figure 5. Distributions of concentrations of various ions, O₂, and H₂, pH and pH* in the middle of a crevice.

concentration of H^+ , pH^* is the modified pH by Y_{all} , which presents a good agreement with the experimental values. The detailed information for the activity coefficients can be found in earlier literatures [4,13].

2) Simulation on change of chemical species with progress of crevice corrosion

The simulation on change of chemical species with progress of corrosion in a crevice as shown in Fig. 1, is conducted by an external constant potential of -0.2 V v.s. SHE. The equilibrium reactions shown in Table 1 and the electrochemical reactions shown in eqs. (7)-(9) are involved, in which the equilibrium potentials, $E_{eq,S}$ for eqs. (8) and (9) are considered as a function of pH and pH^* [11].

$$E_{eq,O_2} = 1.228 - 0.059 \times pH, \quad (11)$$

$$E_{eq,H_2} = -0.059 \times pH^*. \quad (12)$$

$c_{O_2,bulk}=0.16$ mol/m³ and $c_{H_2,bulk}=1.0$ mol/m³ are used.

The results at 100 hours after corrosion are presented in Figs. 4-6. The dissolved Fe^{2+} , Ni^{2+} , and Cr^{3+} ions largely fill in the crevice. The maximum concentrations of Fe^{2+} , Ni^{2+} , and Cr^{3+} ion reach 206 mol/m³, 188 mol/m³, 34 mol/m³, respectively. pH decreases from the initial value of 6 to 2.5 and also the modified value pH^* by activity coefficient decreases to 0.5. Chloride ions (Cl^-) penetrate into the crevice from the external solution and a maximum concentration of 4000 mol/m³ is reached. It is obvious that a high concentration distribution of Cl^- is formed in the crevice. It is also found that dissolved oxygen is consumed in the crevice and the amount of invasion due to diffusion is so small that almost no dissolved oxygen exists inside the crevice.

Figure 5 shows the distributions of concentrations of various ions, O_2 , and H_2 , pH and pH^* in the middle of the crevice. Since the dissolved current density in the entrance of crevice is high according to polarization curves, the concentration of Fe^{2+} appears a maximum value in the entrance of crevice. The evolved hydrogen concentration appears a quasi-uniform distribution inside the crevice, but the oxygen concentration has a dramatic decrease in the crevice, which is lower than 1×10^{-13} mol/m³ in the interior area of crevice.

In calculation, it is found that it would take a while to reach the equilibrium state in corrosion as shown in Fig. 6. It is not easy for the present model to obtain a converged solution by using the Equilibrium Reaction function provided in the Tertiary

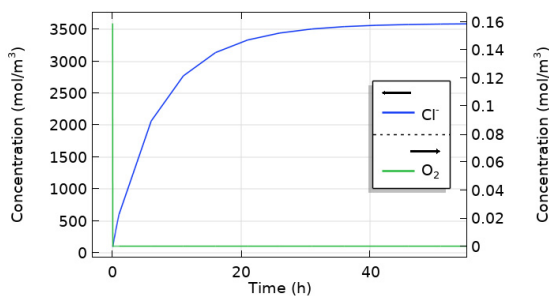


Figure 6. Time variation of concentrations of Cl^- ion and O_2 .

Current Distribution, Nernst-Planck interface of COMSOL Multiphysics®. In order to improve the convergence, the Chemistry interface is used to perform the calculation of equilibrium reactions. As shown in Fig. 6, the Cl^- concentration reaches the equilibrium state in 40 hours after corrosion. The combined approach of the Chemistry interface and the Tertiary Current Distribution, Nernst-Planck interface is verified in this work. It is also noted that since a high concentration distribution of Cl^- is formed, in calculation the obtained Na^+ concentration sometimes becomes negative by the electroneutrality condition shown in eq. (4). This will be further studied in near future.

Conclusions

In this paper, the simulation of crevice corrosion of SUS304 stainless steel in NaCl solution is performed using COMSOL Multiphysics®. The change in solution properties due to crevice corrosion is obtained and analyzed. An efficient approach is proposed to calculate the temporal change of chemical reactions in solution until an equilibrium state is reached. Calculation of transport of various chemical species and chemical and electrochemical reactions inside the crevice, indicates that a highly accurate numerical simulation is succeeded. It is expected that the approach proposed in this work could be applied to further elucidate actual complex corrosion phenomena that involve various chemical reactions of solution in near future.

References

1. S.M. Sharland, C.P. Jackson, and A.J. Diver, "A finite-element model of the propagation of corrosion crevices and pits", *Corrosion. Science* **29** (9), 1149-1166 (1989).
2. F.M. Song, "A mathematical model developed to predict the chemistry and corrosion rate in a crevice of variable gap", *Electrochimica Acta* **56**, 6789–6803 (2011).
3. J.C. Walton, "Mathematical modeling of mass transport and chemical reaction in crevice and pitting corrosion," *Corrosion Science* **30** (8/9), 915–928 (1990).
4. Y. Fukaya and T. Shinohara, "Solution characteristics of synthetic liquid in the crevice of stainless steel", *66th Symposium of Materials and Environments in Japan*, B-107 (2019) [in Japanese].
5. L.Z. Tong, "Advanced numerical analysis tool of corrosion and protection: COMSOL Multiphysics®", *Corrosion Engineering* **62** (10), 294–299 (2013).
6. L.Z. Tong, K. Ozawa, and M. Yamamoto, "Numerical analysis of the variation of solution properties inside crevice due to the crevice corrosion using versatile software", *66th Symposium of Materials and Environments in Japan*, B-108 (2019) [in Japanese].
7. J.S. Newman and K.E. Thomas-Alyea: *Electrochemical Systems*, 3rd ed., John Wiley & Sons, Inc., Hoboken, NJ (2004).
8. M. Fukukawa and L.Z. Tong, "Effect of mass flow induced by a reciprocating paddle on electroplating", Proceedings of the 2017 COMSOL Conference in Boston (2017).
9. T. Aoyama, Y. Sugawara, I. Muto, and N. Hara, " NH_4^+ generation: The role of NO_3^- in the crevice corrosion repassivation of type 316L stainless steel", *Journal of The Electrochemical Society* **166** (10) C250-C260 (2019).

10. S.P. Whitea, G.J. Weira, and N.J. Laycock, "Calculating chemical concentrations during the initiation of crevice corrosion", *Corrosion Science* **42**, 605-629 (2000).

11. M. Stern, "The electrochemical behavior, including hydrogen overvoltage, of iron in acid environments", *Journal of The Electrochemical Society* **102** (11), 609-616 (1955).

12. L.Z. Tong, "Tertiary current distributions on the wafer in a plating cell", Proceedings of the 2012 COMSOL Conference in Boston (2012).

13. M. Takahashi, "Role of the thermodynamic properties of concentrated aqueous solutions in corrosion processes", *Corrosion Engineering* **23** (12), 625-637 (1974) [in Japanese].